Published in final edited form as:
Free Radic Biol Med. 2010 July 1; 49(1): 109–116. doi:10.1016/j.freeradbiomed.2010.04.006.

Dihydroorotate dehydrogenase is required for *N*-(4-hydroxyphenyl)retinamide-induced reactive oxygen species production and apoptosis

Numsen Hail Jr.[*], **Ping Chen**, **Jadwiga J. Kepa**, **Lane R. Bushman**, and **Colin Shearn**
Department of Pharmaceutical Sciences, University of Colorado Denver School of Pharmacy, Aurora, Colorado

Abstract

The synthetic retinoid *N*-(4-hydroxyphenyl)retinamide (4HPR) exhibits anticancer activity *in vivo* and triggers apoptosis in transformed cells *in vitro*. Thus, apoptosis induction is acknowledged as a mechanistic underpinning for 4HPR's cancer preventive and therapeutic effects. Apoptosis induction by 4HPR is routinely preceded by and dependent on the production of reactive oxygen species (ROS) in transformed cells. Very little evidence exists outside the possible involvement of the mitochondrial electron transport chain or the plasma membrane NADPH oxidase complex, which would pinpoint the predominant site of 4HPR-induced ROS production in transformed cells. Here, we investigated the role of dihydroorotate dehydrogenase (DHODH, an enzyme associated with the mitochondrial electron transport chain and required for *de novo* pyrimidine synthesis) in 4HPR-induced ROS production and attendant apoptosis in transformed skin and prostate epithelial cells. In premalignant prostate epithelial cells and malignant cutaneous keratinocytes the suppression of DHODH activity by the chemical inhibitor teriflunomide or the reduction in DHODH protein expression by RNA interference markedly reduced 4HPR-induced ROS generation and apoptosis. Conversely, colon carcinoma cells that lacked DHODH expression were markedly resistant to the prooxidant and cytotoxic effects of 4HPR. Together, these results strongly implicate DHODH in 4HPR-induced ROS production and apoptosis.

Keywords

N-(4-hydroxyphenyl)retinamide; 4HPR; fenretinide; dihydroorotate dehydrogenase; teriflunomide; reactive oxygen species; apoptosis; mitochondria

Introduction

The vast majority of the *in vitro* studies conducted to date indicate that the putative anticancer effects of the synthetic retinoid *N*-(4-Hydroxyphenyl)retinamide (4HPR, also known as fenretinide) are dependent on its ability to engage apoptosis pathways in transformed cells.

[*]**Corresponding author:** Numsen Hail, Jr., Department of Pharmaceutical Sciences, University of Colorado Denver School of Pharmacy, C238-P15 Research 2, 12700 E. 19th Avenue, Room 3008, Aurora, CO 80045. Telephone: 303-724-6122; Fax: 303-724-7266; Numsen.Hail@UCDenver.edu..

Moreover, nearly all of these studies have shown 4HPR's controlling apoptogenic feature to be the production of reactive oxygen species (ROS, reviewed in [1]). Indeed, 4HPR-induced ROS production has been designated as the causal factor for triggering a panoply of anomalous cellular events including enhanced ceramide production, diminished mitochondrial bioenergetics, the induction of the mitochondrial permeability transition, the up-regulation of death receptors, endoplasmic reticulum stress, lysosomal disruption, increased stress kinase signal transduction, the induction of proapoptotic BCL-2 family members and the suppression of antiapoptotic BCL-2 family members, and the initiation of the DNA damage response, to name a few, which presumably regulated the effector phase of cell death in these transformed cells [1].

There are numerous effectors of apoptosis; all of which ultimately contribute to the degradation and demise of the target cell. Many of these effector mechanisms are directly or indirectly regulated by augmented intracellular ROS [2]. Since the common element associated with 4HPR-induced apoptosis appears to be its initiation by increased intracellular ROS production, it seems logical to further distinguish this property [3,4]. After all this should provide an upstream pharmacological target that is uniquely responsible for the putative anticancer effects of 4HPR.

There is limited information in the current literature that points to a biochemical/cell physiological underpinning for the regulation of 4HPR's prooxidant effects in transformed cells *in vitro*. A recent study has shown the suppression of Rac, which is integral to the plasma membrane NADPH oxidase complex, inhibited 4HPR-indiced ROS and, consequently, apoptosis induction in human head and neck squamous cell carcinoma cells [3]. The site or sites of 4HPR-induced ROS generation may differ depending on cell type, since in transformed skin [5], cervical [6], and prostate [4] epithelial cells, leukemia cells [7], and neuroblastoma cells [8] 4HPR appears to redox cycle within the mitochondrial electron transport chain presumably by reacting at a coenzyme Q-binding site [5].

If, in the later scenario, 4HPR were functioning as a general mitochondrial poison [e.g., coenzyme Q antagonists like rotenone and antimycin A that block electron transfer and proton translocation at complex I and complex III, respectively can achieve the general disruption of oxidative phosphorylation (OXPHOS)] to promote ROS and apoptosis in transformed cells *in vivo*, it would seem likely the drug would produce far more adverse side effects than those commonly observed (e.g., night blindness), especially at sites like the liver, nervous system, and muscle where OXPHOS is normally much higher compared to other tissues in the body. However, it is certainly possible 4HPR could promote ROS at a site associated with OXPHOS that is specifically required in rapidly dividing cells like transformed cells, and not by disrupting OXPHOS in general. This would be exceptionally important because it would not only link 4HPR-induced ROS and apoptosis to OXPHOS, which we have shown previously [4,5], but specifically couple 4HPR's cytotoxic anticancer effects with a process specific to OXPHOS that is required in rapidly proliferating cells like transformed cells.

Thus, we investigated the prospect that dihydroorotate dehydrogenase (DHODH), an enzyme associated with mitochondrial electron transport and required for *de novo* pyrimidine synthesis [9], could be an important link between mitochondrial bioenergetics, cell proliferation, and sensitivity to 4HPR-induced ROS and apoptosis in certain transformed cell types. This study presents evidence that strongly implicates DHODH in 4HPR-induced ROS production and apoptosis induction in transformed skin and prostate epithelial cells. Our *in vitro* mechanistic findings imply that transformed cells relying on DHODH and *de novo* pyrimidine synthesis to sustain aberrant cell proliferation should be responsive to the apoptogenic anticancer effects of 4HPR, which could be advantageous in estimating the potential clinical anticancer efficiency of 4HPR at various sites *in vivo*.

Experimental procedures

Cell culture and reagents

The COLO 16, SCC-13, SRB-1, SRB-12, LNCaP, and PC-3 cell lines were kindly provided by Dr. Reuben Lotan (University of Texas M. D. Anderson Cancer Center, Houston, TX). The DU-145, HaCaT, PWR-1E, and SW480 cell lines were kindly provided by Dr. Rajesh Agarwal (University of Colorado Denver School of Pharmacy, Aurora, CO). The PWR-1E, HaCaT, COLO 16, SCC-13, SRB-1, and SRB-12 cells were cultured in keratinocyte growth medium (KGM), consisting of keratinocyte basal medium supplemented with 100 ng/ml human recombinant epidermal growth factor, 0.4% bovine pituitary extract (all from Invitrogen Corporation, Carlsbad, CA). For the PWR-1E cells, 1 nM of the synthetic androgen R1881 (purchased from Perkin Elmer, Waltham, MA) was also added to the KGM as described previously [4]. The DU-145 LNCaP, PC-3, and SW480 cells were cultured in 1:1 Dulbecco's Modified Eagle's medium/Ham's F12 (DMEM/F12) medium supplemented with 2% fetal bovine serum (Invitrogen). All of the cell cultures were incubated at 37°C in humidified air containing 5% CO_2. Treatments with 4HPR and other agents were performed on sub-confluent cultures.

4HPR was kindly provided by Dr. James A. Crowell (Division of Cancer Prevention, National Cancer Institute, Bethesda, MD). Dimethyl sulfoxide (Me_2SO), 2',7'-dichlorofluorescin diacetate, hydrogen peroxide (H_2O_2) 30% solution, propidium iodide (PI), and leflunomide (LFN) were purchased from Sigma-Aldrich Chemical Co. Teriflunomide (TFN) was purchased from EMD Chemicals (Gibbstown, NJ). Hoechst 33342 (10 mg/ml solution) was purchased from Invitrogen. Brequinar (BQR, NSC 368390) was kindly provided by Dr. Ven L. Narayanan (Drug Synthesis and Chemistry Branch, Division of Cancer Treatment and Diagnosis, National Cancer Institute, Bethesda, MD).

Quantitative cell cycle evaluation and apoptosis assays

Cellular DNA fragmentation was ascertained by flow cytometry using a hypotonic solution of PI [4]. The flow cytometry procedures were performed by a Beckman Coulter FC500 flow cytometer with CXP software (Beckman Coulter, Inc., Fullerton, CA). This procedure was also used to examine the cellular DNA content of viable cells relative to their cell cycle progression. The PI histograms were analyzed by ModFit LT version 3.2 software (Verity Software House, Inc., Topsham, ME), which modeled the cell cycle and provided the percentage of G_0/G_1, S, and G_2/M phase cells in each sample.

Nuclear condensation/fragmentation was assessed by Hoechst 33342 staining and epifluorescence microscopy. The nuclei in six random microscopic fields magnified at 400X were counted for COLO 16 cells cultured in the wells of 6-well tissue culture plates following the indicated treatments. The condensed/fragmented nuclei were expressed as a percentage of the total nuclei counted in each field.

Continuous determination of short-term ROS generation

The cells in 6-well tissue culture plates were washed twice with 2 ml of Krebs-Ringer buffer (KRB, Sigma-Aldrich) and covered with 2 ml of KRB containing 10 μg/ml 2',7'-dichlorofluorescin diacetate and the indicated agent(s) or Me_2SO (control). Fluorescence emission at 538 nm (representing 2',7'-dichlorofluorescein (DCF) production) was measured immediately following mixing (time zero) and subsequently at 30-min intervals over a 150-min period using a SpectraMax Gemini EM dual-scanning microplate spectrofluorimeter (Molecular Devices, Sunnyvale, CA) [4].

Assessment of the uridine concentration in cultured cells

A modified version of a method publish previously [10] was used to characterize the uridine content in cultured cells. Briefly, approximately 2×10^6 cells were lysed in 500 μL of a 70% methanol/deionized water solution (v/v), and the cell debris was then removed via centrifugation. The resulting supernatant was passed through a Waters QMA Accell Plus anion-exchange, solid-phase extraction cartridge (Waters Division, Milford, MA) and the nucleotides were eluted from the cartridge with a 1 M KCl solution. Sweet potato type XA acid phosphatase (5 units, Sigma-Aldrich) in acetate buffer was added to the eluent to dephosphorylate the nucleotides. The samples were desalted and concentrated by a second solid-phase extraction that utilized a Phenomenex Strata X cartridge (Phenomenex, Torrance CA). The methanol eluant from this extraction was dried under nitrogen gas and then reconstituted in 100 μL of deionized water.

The samples were analyzed using a Waters Acquity ultra high-performance liquid chromatograph (Waters Division). The total uridine in the samples was quantified using the characteristic UV absorption (i.e., 260 nm) and retention time obtained from uridine standards (Sigma-Aldrich) ranging from 5 to 500 ng (i.e., the amount injected on column). The standards were processed in the same manner as the cell samples (i.e., anion-exchange, solid-phase extraction, and acid phosphatase digestion).

Measurement of oxygen consumption in cultured cells

Oxygen consumption was measured polarographically using a Clark-type oxygen electrode and YSI Model 5300A Biological Oxygen Monitor (Yellow Spring Instrument Co., Yellow Springs, OH) [4].

Epifluorescence microscopy

Cells cultured in 10 cm or 6-well tissue culture plates were imaged as described previously [4]. A staining solution of 5 μg/ml Hoechst 33342 in KRB at 37°C was used to visualize the nuclear changes associated with apoptosis following the specified treatments. The cells were photographed using a Nikon TE2000 inverted epifluorescence microscope and digital color camera (Nikon Instruments, Melville, NY). Triplicate wells were used for each treatment.

Cell transfection with small interfering RNA (siRNA) and plasmids

SMARTpool siRNA against DHODH and a non-targeting siRNA were synthesized by Dharmacon RNAi Technologies (Lafayette, CO). COLO 16 cells were transfected with the siRNAs using Lipofectamine 2000 (Invitrogen) according to the manufacture's instructions. Briefly, ~2×10^5 cells suspended in 2 ml of KGM were added to the wells of 6-well tissue culture plates. After 24 h, the KGM was removed and replaced with fresh of KGM containing Lipofectamine 2000 and the non-targeting siRNA (siRNA control) or the SMARTpool siRNA against DHODH (siDHODH). The final concentration of siRNA was 200 pmol/well. After 24 h, the cells were washed with KRB containing 2% albumin (Sigma-Aldrich) to remove the excess Lipofectamine 2000, and new KGM was added for additional 24-h incubation after which the COLO 16 cells were evaluated for 4HPR-induced ROS or apoptosis. DHODH protein suppression was ascertained 48 h post transfection by immunoblot analysis.

We also transfected the SW480 cells as described above with an expression vector encoding DHODH, green fluorescent protein, or an empty vector control (Open Biosystems, Huntsville, AL). DMEM/F12 medium without 2% fetal bovine serum was used for the initial 24-h transfection of the SW480 cells. A 48-h assessment of the transfection efficiency using epifluorescence microscopy to detect cellular green fluorescent protein expression revealed that roughly 28% of the SW480 received the green fluorescent protein expression vector. The

SW480 cells were subjected to analysis for DHODH expression, 4HPR-induced ROS, and 4HPR-induced apoptosis in the same manner described above for the COLO 16 cells 48 h following transfection.

Immunoblotting

Cellular proteins were characterized as described previously [4]. The membranes were probed with the antibodies for the human proteins DHODH (purchased from Sigma-Aldrich), cytochrome *c* oxidase (i.e., complex IV) subunit 2 (COII, purchased from Invitrogen), the NADH ubiquinone oxidoreductase (i.e., complex I) subunit 6 (ND6, purchased from Invitrogen), or β-actin (purchased from Santa Cruz Biotechnology, Santa Cruz, CA). The binding of the primary antibody was detected with a horseradish peroxidase-linked secondary antibody using an enhanced chemiluminescence kit (Amersham Biosciences Corp., Piscataway, NJ). Immunoblots were subjected to densitometric analysis using ImageJ software (National Institutes of Health, Bethesda, MD). The band intensity of DHODH, ND6, and COII were normalized as a percent of the loading control β-actin.

Statistical analyses

The statistical significance between the means of two groups or more was determined using a two-sided, unpaired *t* test or a one-way ANOVA with Dunnett's post test, respectively (GraphPad InStat version 3.0 software, GraphPad Software, Inc., San Diego, CA). Where indicated, the results are expressed as the mean value of triplicate samples ± SD (error bars). All means ± S.D. for triplicate samples were calculated with Microsoft Excel 2003 SP2 software (Microsoft Corporation, Seattle, WA). In all statistical analyses, the results were considered significant for $P<0.05$.

Results and discussion

DHODH is expressed in premalignant and malignant skin and prostate epithelial cells

De novo pyrimidine synthesis is indispensable in rapidly proliferating cells in order to meet their increased demand for nucleic acid precursors, and this pathway is believed to be essential for aberrant cell proliferation following cell transformation [9]. DHODH is located in the inner mitochondrial membrane where it serves as the rate-limiting enzyme in the *de novo* pathway of pyrimidine synthesis. Coenzyme Q is the proximal electron acceptor for dihydroorotate's oxidation to orotate by DHODH. Oxygen functions as the ultimate electron acceptor for this reaction via electron transfer at complex IV. In this scenario, dihydroorotate acts as a reducing equivalent like NADH or succinate to modulate OXPHOS (Fig. 1A).

We examined DHODH expression in the premalignant HaCaT keratinocytes and the COLO 16, SCC-13, SRB-1, and SRB-12 cutaneous squamous cell carcinoma cells. Among these cells, DHODH was consistently expressed (Fig. 1B). The level of DHODH expression among the cutaneous keratinocytes was similar to that observed in the premalignant PWR-1E and malignant DU-145, LNCaP, and PC-3 prostate epithelial cells (Fig. 1C).

The chemical inhibition of DHODH activity or the reduction of DHODH protein suppresses 4HPR-induced ROS production and apoptosis in transformed skin and prostate epithelial cells

Teriflunomide (TFN) is a redox silent coenzyme Q antagonist of DHODH. TFN inhibits the proliferation of mitogen-activated T-cells, which is believed to the mechanistic basis for its antirheumatic activity *in vivo* [11]. Interestingly, TFN shares a chemical similarity with 4HPR (Fig. 2A). The notable difference between these two chemicals regarding their potential redox activity would be the presumed redox silent trifluoromethylphenyl moiety of TFN versus the phenolic moiety of 4HPR. We have previously proposed that 4HPR-induced ROS production

likely originates via a phenoxyl radical that is generated by an enzymatic process occurring at a coenzyme Q-binding site in the mitochondrial electron transport chain [5].

In vitro characterizations of TFN's activity in epithelial cells are limited. A short-term *in vitro* 50 μM TFN treatment caused the suppression of DNA synthesis and cell cycle arrest in multiple myeloma cells [12]. We observed a marked suppression of cell proliferation in the COLO 16 and PWR-1E cells (not shown), an accumulation of these cells in the S phase of the cell cycle (Fig. 2B), and a ≥50% suppression in their cellular uridine concentration (Fig. 2C) compared to the respective control cells following a 24-h exposure to 50 μM TFN. There was no obvious change in the expression of DHODH protein in these cells after a 24-h exposure to TFN (Fig. 2D). Together, these results illustrated that a short-term (i.e., ≤24 h) exposure to TFN could repress DHODH enzymatic activity in transformed epithelial cells.

The modulation of DHODH by TFN in the COLO 16 and PWR-1E cells should also suppress the overall mitochondrial function in these cells. Indeed, a short-term 4-h exposure to 50 μM TFN caused roughly a 25 to 30% reduction in the oxygen consumption in the COLO 16 and PWR-1E cells, respectively (Fig. 3A). A 4-h pretreatment with TFN also suppressed ~90% of the 4HPR induced ROS production as measured by the oxidation of 2',7'-dichlorofluorescin to DCF in the PWR-1E cells. This effect was apparently not due to ROS scavenging by TFN, since this agent had no influence on the DCF production triggered by H_2O_2. The kinetics of the DCF production caused by 4HPR and H_2O_2 were quite different and suggested that the 4HPR-induced ROS production, and its repression by TFN, were potentially linked to an enzymatic process in the PWR-1E cells (Fig. 3B).

The TFN pretreatment caused a similar suppression of the DCF production in the COLO 16 cells, and LFN, the prodrug of TFN, suppressed the 4HPR-induced ROS production by roughly 30% (Fig. 3C). This partial suppression of the 4HPR-induced ROS production by LFN relative to TFN was anticipated since in LFN is slowly hydrolyzed non-enzymatically to yield TFN in aqueous solutions [13]. An equal molar concentration of the prototypical DHODH inhibitor BQR [14] suppressed 4HPR-induced ROS production comparable to that observed by TFN (Fig. 3B). Moreover, TFN mediated a 90% or greater inhibition of ROS production by 4HPR in the premalignant HaCaT keratinocytes and the malignant DU-145 prostate epithelial cells (Fig. 3D). We have observed a comparable inhibition of 4HPR-induced ROS production in respiration deficient skin [5] and prostate [4] epithelial cells that consume roughly 10% of the oxygen of their parental counterparts. Since the 4-h exposure to TFN only suppressed roughly 30% of the oxygen consumption by the COLO 16 or PWR-1E cells, we would consider the conspicuous short-term outcome of TFN's repression of 4HPR-induced ROS production in these cells to be biologically significant. It is also important to note that the DHODH inhibitors alone suppressed ≥50% of the constitutive ROS production in the transformed skin and prostate epithelial cells, which would portray DHODH as a biologically significant source of ROS [15] in these cells.

Reports from our group and others have shown short-term (i.e., within 48 h) sensitivity to 4HPR (i.e. 5 to 10 μM) induced apoptosis in skin [5,16,17] and prostate [4,18-20] epithelial cells. In fact, we have reported that 12- to 24-h exposures to 5 μM 4HPR were quite effective in triggering conspicuous (i.e., occurring in ~50% or more of the treatment populations) cell death in transformed skin [17] and prostate [4] epithelial cells. A 4-h pretreatment with TFN blocked the morphological changes (i.e., cell shrinkage and nuclear condensation/fragmentation) caused by a subsequent 24-h exposure to 5 μM 4HPR in the COLO 16 cells (Fig. 4A), and markedly suppressed the development of hypoploid cells following a similar exposure in the PWR-1E cells (Fig 4B). A summary of the percent hypoploid cells detected in triplicate samples of the COLO 16 and PWR-1E cells exposed for 24 h to TFN, 4HPR, TFN and 4HPR, or Me_2SO (control) is presented in Fig. 4C.

We wanted to determine if the suppression of DHODH protein expression would also inhibit 4HPR-induced ROS levels and apoptosis in the COLO 16 cells. Using a pool of four siRNAs against DHODH mRNA translation we transfected the COLO 16 cells and examined them for 4HPR-induced ROS production. Following a 48-h siDHODH treatment we were able to suppress the short-term 4HPR-induced ROS production by roughly 75% relative to the non-targeting siRNA control cells exposed to 4HPR (Fig. 5A). The siDHODH also attenuated DHODH protein expression by ~60% compared to the siRNA control (Fig. 5A, inset). Similarly, the siDHODH blocked the 24-h 4HPR-induced cell death in the COLO 16 cells as evidenced by the conspicuous suppression of nuclear condensation and fragmentation in this cell population compared to the siRNA control population (Fig. 5B). A summary of the percent condensed and fragmented nuclei in the indicated treatment populations is presented in Fig. 5C. Together, these results implicate DHODH in 4HPR-induced ROS and apoptosis in transformed skin and prostate epithelial cells.

Colon cancer cells lacking DHODH expression exhibit resistance to 4HPR-induced ROS production and apoptosis

A recent study has shown several colon cancer cell lines are markedly resistant 4HPR-induced apoptosis [21]. We too observed the SW480 colorectal adenocarcinoma cells ware especially resistant to 4HPR-induced apoptosis. Treating these cells with 5 or 10 μM 4HPR for 24, 48, or 72 h was apparently unable to trigger a conspicuous amount of hypoploid cell formation in the treatment populations (Fig. 6A). Interestingly, the 72-h treatment with 10 μM 4HPR altered the cell cycle distribution in the SW480 cells. There were roughly 13% more cells in the S and G_2/M phases of the cell cycle compared to the Me_2SO-treated control cells (Fig. 6A, inset).

The SW480 cells were susceptible to a conspicuous apoptosis induction triggered by a short-term, 24-h exposure to the rotenoid cancer chemopreventive agent deguelin, which is a complex I inhibitor [22] (Fig. 6A). This would suggest that the general disruption of OXPHOS resulted in cytotoxicity in these cells. We have noted a similar apoptotic response to deguelin in COLO 16 and SRB-12 cells [22].

Immunoblot analysis revealed that the SW480 cells had little or no DHODH expression compared to the PWR-1E or COLO 16 cells (Fig. 6B). Interestingly, the UniGene database (National Center for Biotechnology Information, U.S. National Library of Medicine, Bethesda, MD) illustrates that expressed sequence tags (ESTs, i.e., mRNA) for human DHODH have not been detected in colorectal tumor tissues. The relative levels of DHODH ESTs detected in skin and prostate tumors were roughly twice that observed in their respective normal tissue counterparts, and generally elevated (i.e., about thee-fold) ESTs have been detected in non-neoplastic (e.g., premalignant) tissues relative to normal tissues (http://www.ncbi.nlm.nih.gov/UniGene/ESTProfileViewer.cgi?uglist=Hs.654427).

We also examined ND6 (found in complex I) and COII (found in complex IV) protein expression in the PWR-1E, COLO16, and SW480 cells, and observed no obvious differences in the expression levels of these respiratory chain subunits among the PWR-1E, COLO16, and SW480 cells (Fig. 6B). Moreover, the SW480 cells had less than a two-fold increase in 4HPR-induced ROS production compared to the roughly seven-fold increase observed in the PWR-1E cells. Although the short-term 4HPR-induced ROS production was statistically significant in both the PWR-1E and SW480 cells, its biological significance with respect to a conspicuous induction of apoptosis could not be demonstrated in the SW480 cells.

We successfully increased DHODH protein expression by roughly 35 fold in the SW480 cells following a 48-h transfection using a plasmid for the full-length human DHODH gene sequence. This level of DHODH expression was comparable to that observed in the COLO 16 cells. However, this increase in DHODH expression did not equate to a heightened sensitivity

to 4HPR-induced ROS or apoptosis in the SW480 cells. We were unable to detect any obvious changes in this regard following a 48- or 72-h DHODH transfection (not shown), which may be due, at least in part, to the relatively low (i.e., ~28%) transfection efficiency in these epithelial cells (please see the experimental procedures section). It is also important to note that DHODH is the fourth of six enzymes in the *de novo* pyrimidine synthesis pathway. The other five enzymes in this pathway constitute two different enzyme complexes located in the cytoplasm. The first three enzymes form the multienzyme complex CAD, and the fifth and sixth enzymes form the UMP synthase [23]. Thus, it is conceivable the absence of one or more the constituents of these multifunctional enzyme complexes could have rendered the *de novo* pathway for pyrimidine synthesis inactive in the DHODH transfected SW480 cells, which could account for their enduring resistance to 4HPR's prooxidant and apoptogenic effects. Furthermore, enterocytes normally salvage nucleosides for potential systemic use from nutrients passing through the gut. These salvaged nucleosides can regulate proliferation in these cells [24]. Accordingly, the *de novo* pyrimidine synthesis pathway may not be essential to support cell proliferation in this particular cell type.

The data presented here implicate DHODH as a prominent determinant in 4HPR-induced ROS and apoptosis in transformed skin and prostate epithelial cells. Our findings would also suggest that DHODH is an important constituent of OXPHOS and cell proliferation in these cells. Anomalous cell proliferation in premalignant cells is required for their promotion and progression to a malignant phenotype. Thus, we believe DHODH could be an essential constituent in skin and prostate tumorigenesis, and a crucial target in 4HPR-mediated skin and prostate cancer chemoprevention or therapy. Given these results and those we [4,5] and others [8] have published previously using respiration-deficient cells, which exhibit resistance to 4HPR-induced ROS and apoptosis, are pyrimidine auxotrophs, and whose metabolic characteristics (i.e., they utilize glycolytic metabolism over oxidative metabolism) *in vitro* could emulate tumor cell growth under hypoxic conditions *in vivo* [4], we would speculate that 4HPR would be most effective in skin or prostate cancer chemoprevention. Kadara *et al*. suggested that malignant human head and neck squamous cell carcinoma cells were potentially more sensitive to 4HPR-induced ROS and apoptosis than their primary head and neck squamous cell carcinoma cell counterparts due to their higher degree of Rac activation by 4HPR [3]. These distinct characteristics of 4HPR-induced ROS and apoptosis may indeed be tissue specific as we alluded to previously. It is also essential to note that the evaluation of proteins like Rac and DHODH in the target tissue of prospective patients who might benefit from 4HPR in a clinical setting could conceivably improve the overall efficacy of this chemical agent irrespective of whether this improvement occurs in the arena of cancer prevention or therapy. Additional studies are certainly warranted to investigate these possibilities further.

Acknowledgments

this work was supported by funds provided by the National Cancer Institute (grant number CA133901-01 to N. Hail, Jr.) and the University of Colorado Denver School of Pharmacy. We thank Christine Childs with the University of Colorado Cancer Center Flow Cytometry Core for her assistance with the acquisition of the flow cytometry data presented in this study.

Abbreviations used

4HPR	*N*-(4-hydroxyphenyl)retinamide
BQR	brequinar
DCF	2',7'-dichlorofluorescein
DHODH	dihydroorotate dehydrogenase
ESTs	expressed sequence tags

FU	fluorescence units
H_2O_2	hydrogen peroxide
KGM	keratinocyte growth medium
KRB	Krebs-Ringer buffer
LFN	leflunomide
Me_2SO	dimethyl sulfoxide
OXPHOS	oxidative phosphorylation
PI	propidium iodide
ROS	reactive oxygen species
siRNA	small interfering RNA
TFN	teriflunomide

References

1. Hail N Jr. Kim HJ, Lotan R. Mechanisms of fenretinide-induced apoptosis. Apoptosis 2006;11:1677–1694. [PubMed: 16850162]
2. Hail N Jr. Carter BZ, Konopleva M, Andreeff M. Apoptosis effectors mechanisms: a requiem performed in different keys. Apoptosis 2006;11:889–904. [PubMed: 16547589]
3. Kadara H, Tahara E, Kim HJ, Lotan D, Myers J, Lotan R. Involvement of Rac in fenretinide-induced apoptosis. Cancer Res 2008;68:4416–4423. [PubMed: 18519704]
4. Hail N Jr. Chen P, Kepa JJ. Selective apoptosis induction by the cancer chemopreventive agent *N*-(4-hydroxyphenyl)retinamide is achieved by modulating mitochondrial bioenergetics in premalignant and malignant human prostate epithelial cells. Apoptosis 2009;14:449–863.
5. Hail N Jr. Lotan R. Mitochondrial respiration is uniquely associated with the prooxidant and apoptotic effects of *N*-(4-hydroxyphenyl)retinamide. J. Biol. Chem 2001;276:45614–45621. [PubMed: 11546781]
6. Suzuki S, Higuchi M, Proske RJ, Oridate N, Hong WK, Lotan R. Implication of mitochondria-derived reactive oxygen species, cytochrome *c* and caspase-3 in *N*-(4-hydroxyphenyl)retinamide-induced apoptosis in cervical carcinoma cells. Oncogene 1999;18:6380–6387. [PubMed: 10597238]
7. Asumendi A, Morales MC, Alvarez A, Arechaga J, Perez-Yarza G. Implication of mitochondria-derived ROS and cardiolipin peroxidation in *N*-(4-hydroxyphenyl)retinamide-induced apoptosis. Br. J. Cancer 2002;86:1951–1956. [PubMed: 12085192]
8. Cuperus R, Leen R, Tytgat GA, Caron HN, van Kuilenburg AB. Fenretinide induces mitochondrial ROS and inhibits the mitochondrial respiratory chain in neuroblastoma. Cell. Mol. Life Sci 2010;67:807–816. [PubMed: 19941060]
9. Evans DR, Guy HI. Mammalian pyrimidine biosynthesis: Fresh insights into an ancient pathway. J. Biol. Chem 2004;279:33035–33038. [PubMed: 15096496]
10. Fletcher CV, Kawle SP, Kakuda TN, Anderson PL, Weller D, Bushman LR, Brundage RC, Remmel RP. Zidovudine triphosphate and lamivudine triphosphate concentration-response relationships in HIV-infected persons. AIDS 2000;14:2137–2144. [PubMed: 11061655]
11. Davis JP, Cain GA, Pitts WJ, Magolda RL, Copeland RA. The immunosuppressive metabolite of leflunomide is a potent inhibitor of human dihydroorotate dehydrogenase. Biochemistry 1996;35:1270–1273. [PubMed: 8573583]
12. Baumann P, Mandl-Weber S, Volkl A, Adam C, Bumeder I, Oduncu F, Schmidmaier R. Dihydroorotate dehydrogenase inhibitor A771726 (leflunomide) induces apoptosis and diminishes proliferation of multiple myeloma cells. Mol. Cancer Ther 2009;8:366–375. [PubMed: 19174558]
13. Tallantyre E, Evangelou N, Constantinescu CS. Spotlight on teriflunomide. Int. MS J 2008;15:62–68. [PubMed: 18782502]

14. Peters GJ, Schwartsmann G, Nadal JC, Laurensse EJ, van Groeningen CJ, van der Vijgh WJ, Pinedo HM. *In vivo* inhibition of the pyrimidine *de novo* enzyme dihydroorotic acid dehydrogenase by brequinar sodium (DUP-785; NSC 368390) in mice and patients. Cancer Res 1990;50:4644–4649. [PubMed: 2164443]

15. Forman JH, Kennedy J. Superoxide production and electron transport in mitochondrial oxidation of dihydroorotic acid. J. Biol. Chem 1975;250:4322–4326. [PubMed: 165196]

16. Davies M, Paterson IC, Ganapathy A, Prime SS. Cell death induced by *N*-(4-hydroxyphenyl) retinamide in human epidermal keratinocytes is modulated by TGF-beta and diminishes during the progression of squamous cell carcinoma. Int. J. Cancer 2006;119:2803–2811. [PubMed: 17044020]

17. Hail N Jr. Lotan R. Mitochondrial permeability transition is a central coordinating event in *N*-(4-hydroxyphenyl)retinamide-induced apoptosis. Cancer Epidemiol. Biomarkers Prev 2000;9:1293–1301. [PubMed: 11142414]

18. Hursting SD, Shen JC, Sun XY, Wang TT, Phang JM, Perkins SN. Modulation of cyclophilin gene expression by *N*-4-(hydroxyphenyl)retinamide: association with reactive oxygen species generation and apoptosis. Mol. Carcinog 2002;33:16–24. [PubMed: 11807954]

19. Sun S-Y, Yue P, Lotan R. Induction of apoptosis by *N*-(4-hydroxyphenyl)retinamide and its association with reactive oxygen species, nuclear retinoic acid receptors, and apoptosis related genes in human prostate carcinoma cells. Mol. Pharmacol 1999;55:403–410. [PubMed: 10051523]

20. Hsieh TC, Wu JM. Effects of fenretinide (4-HPR) on prostate LNCaP cell growth, apoptosis, and prostate-specific gene expression. Prostate 1997;33:97–104. [PubMed: 9316650]

21. Kouhara J, Yoshida T, Nakata S, Horinaka M, Wakada M, Ueda Y, Yamagishi H, Sakai T. Fenretinide up-regulates DR5/TRAIL-R2 expression via the induction of the transcription factor CHOP and combined treatment with fenretinide and TRAIL induces synergistic apoptosis in colon cancer cell lines. Int. J. Oncol 2007;30:679–687. [PubMed: 17273769]

22. Hail N Jr. Lotan R. Apoptosis induction by the natural product cancer chemopreventive agent deguelin is mediated through the inhibition of mitochondrial respiration. Apoptosis 2004;9:437–447. [PubMed: 15192326]

23. Peters GJ, Laurensse E, Leyva A, Pinedo HM. A sensitive, nonradiometric assay for dihydroorotic acid dehydrogenase using anion-exchange high-performance liquid chromatography. Anal. Biochem 1987;161:32–38. [PubMed: 3578785]

24. Rodríguez-Serrano F, Marchal JA, Ríos A, Marínez-Amat A, Boulaiz H, Prados J, Perán M, Caba O, Carrillo E, Hita F, Aránega A. Exogenous nucleosides modulate proliferation of rat intestinal epithelial IEC-6 cells. J. Nutr 2007;137:879–884. [PubMed: 17374648]

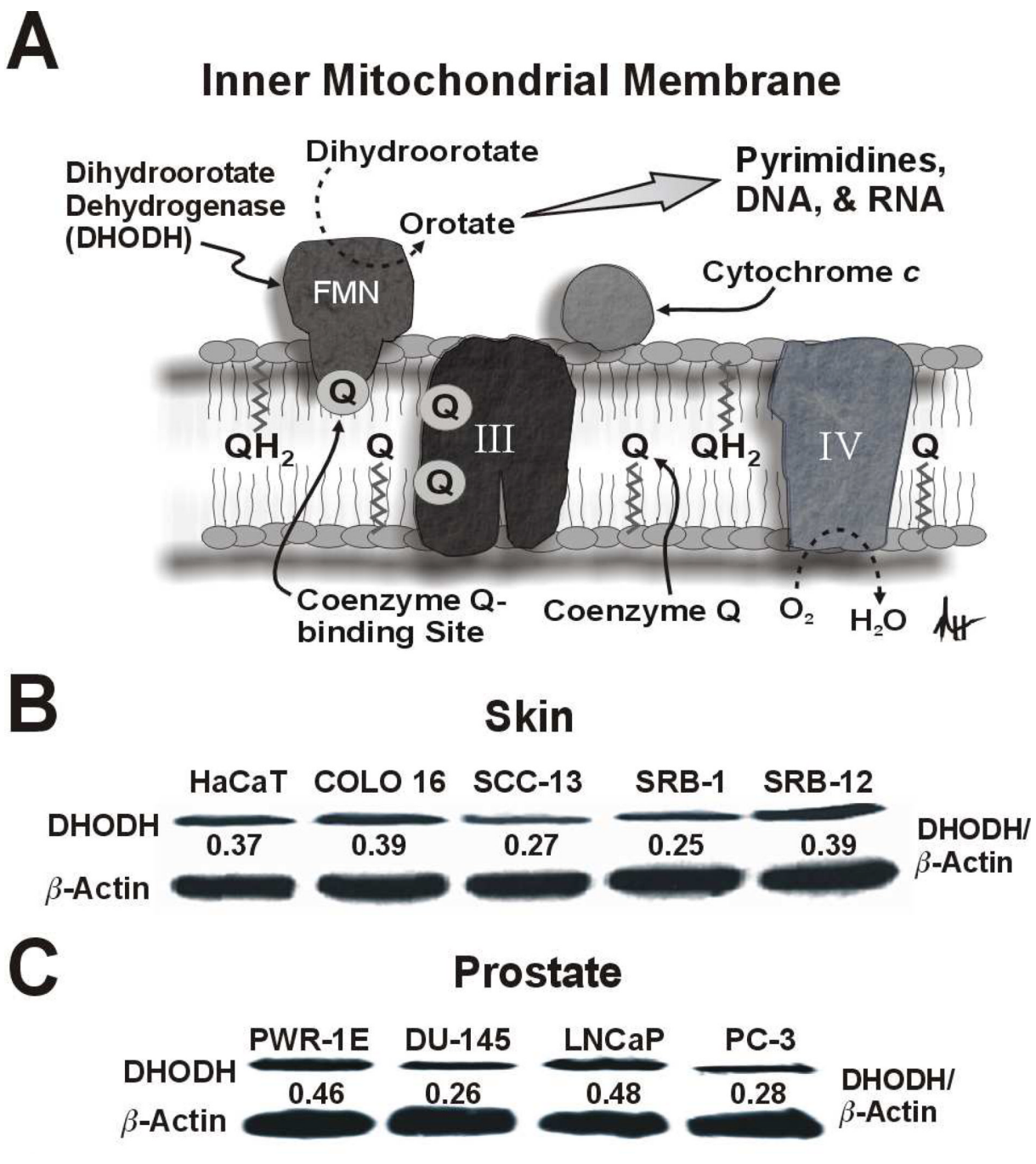

Fig 1.

DHODH protein is expressed in premalignant and malignant human skin and prostate epithelial cells. (A) A diagrammatic depiction of DHODH in the inner mitochondrial membrane illustrating its role in mitochondrial bioenergetics and *de novo* pyrimidine synthesis. Please refer to the text for additional details (abbreviations: III, complex III, IV, complex IV; FMN, flavin mononucleotide). An immunoblot analysis of DHODH expression for the premalignant HaCaT and malignant COLO 16, SCC-13, SRB-1, and SRB-12 cutaneous keratinocytes (B), and the premalignant PWR-1E and malignant DU-145, LNCaP, and PC-3 prostate epithelial cells (C).

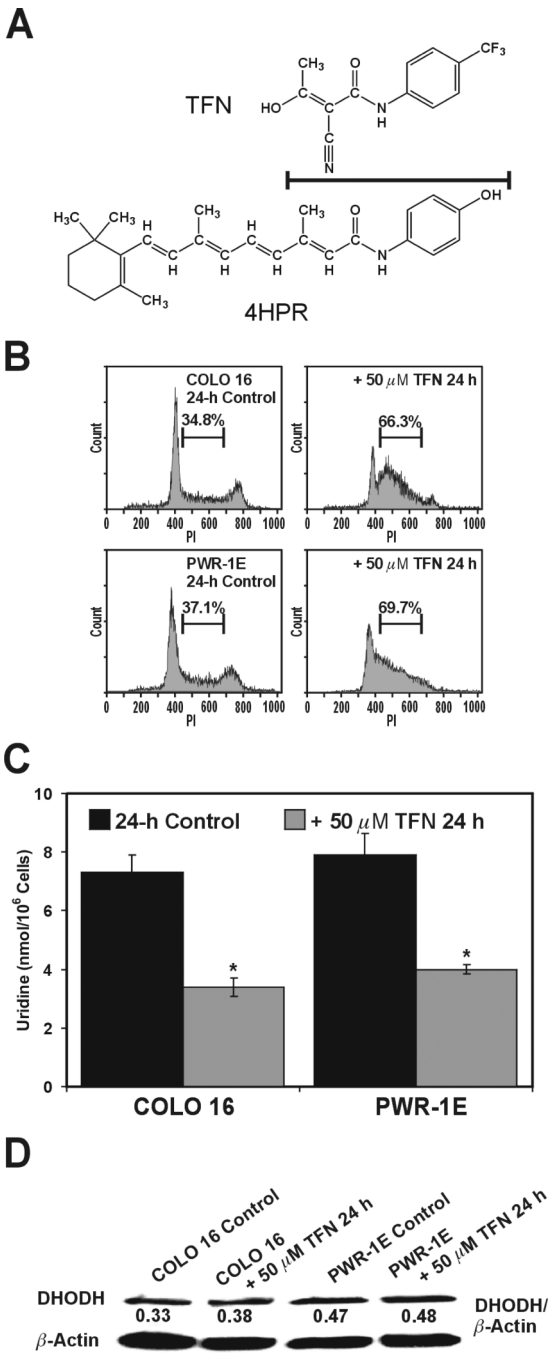

Figure 2.

TFN suppresses DHODH activity in premalignant and malignant human skin and prostate epithelial cells. (A) The chemical structures for TFN and 4HPR. The line separating these structures also designates their chemical similarity. (B) Representative PI histograms showing the percent S phase cells for the COLO 16 and PWR-1E cells exposed for 24 h to Me_2SO (control) or 50 μM TFN. (C) The cellular uridine levels were determined for ~10^6 cells exposed to Me_2SO (control) or 50 μM TFN for 24 h. *P<0.001 compared to the respective controls. (D) An immunoblot analysis of DHODH expression for the COLO 16 and PWR-1E cells exposed to Me_2SO (control) or 50 μM TFN for 24 h.

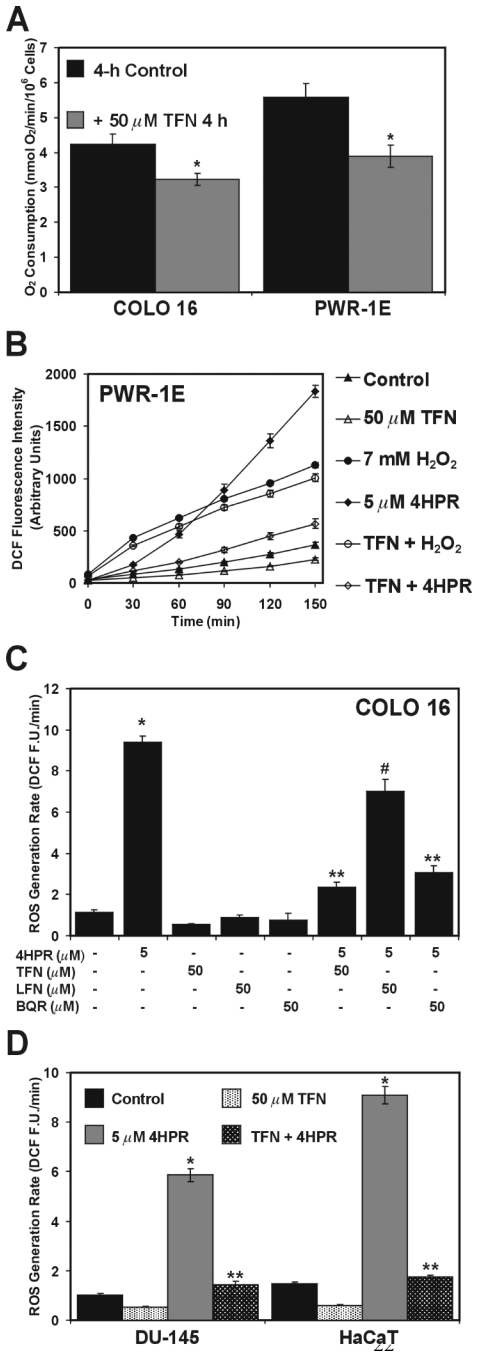

Figure 3.

DHODH inhibitors diminish mitochondrial bioenergetics and 4HPR-induced ROS production in PWR-1E and COLO 16 cells. (A) An assessment of the oxygen consumption in COLO 16 and PWR-1E cells exposed to Me_2SO (control) or 50 μM TFN for 4 h. **P*<0.01 compared to the respective controls. The PWR-1 E (B), COLO 16 (C), DU-145 (D), and HaCaT (D) cells cultured in 6-well tissue culture plates were pretreated for 4 h with the indicated concentration of TFN, LFN, or BQR. The medium was removed and replaced with KRB containing 10 μg/ml 2',7'-dichlorofluorescin diacetate and the indicated concentrations of hydrogen peroxide or 4HPR. The ROS generation rates (fluorescence units/min, F.U./min) in (C) and (D) were derived from the slopes of lines obtained between 30 and 120 min for triplicate wells in 6-well

tissue culture plates. The 6-well tissue culture plates were incubated at 37°C between the 30-min intervals for fluorescence determination. *P<0.001 compared to the respective controls, **P<0.001 compared to the respective 4HPR treatments, and #P<0.01 compared to the respective 4HPR treatment.

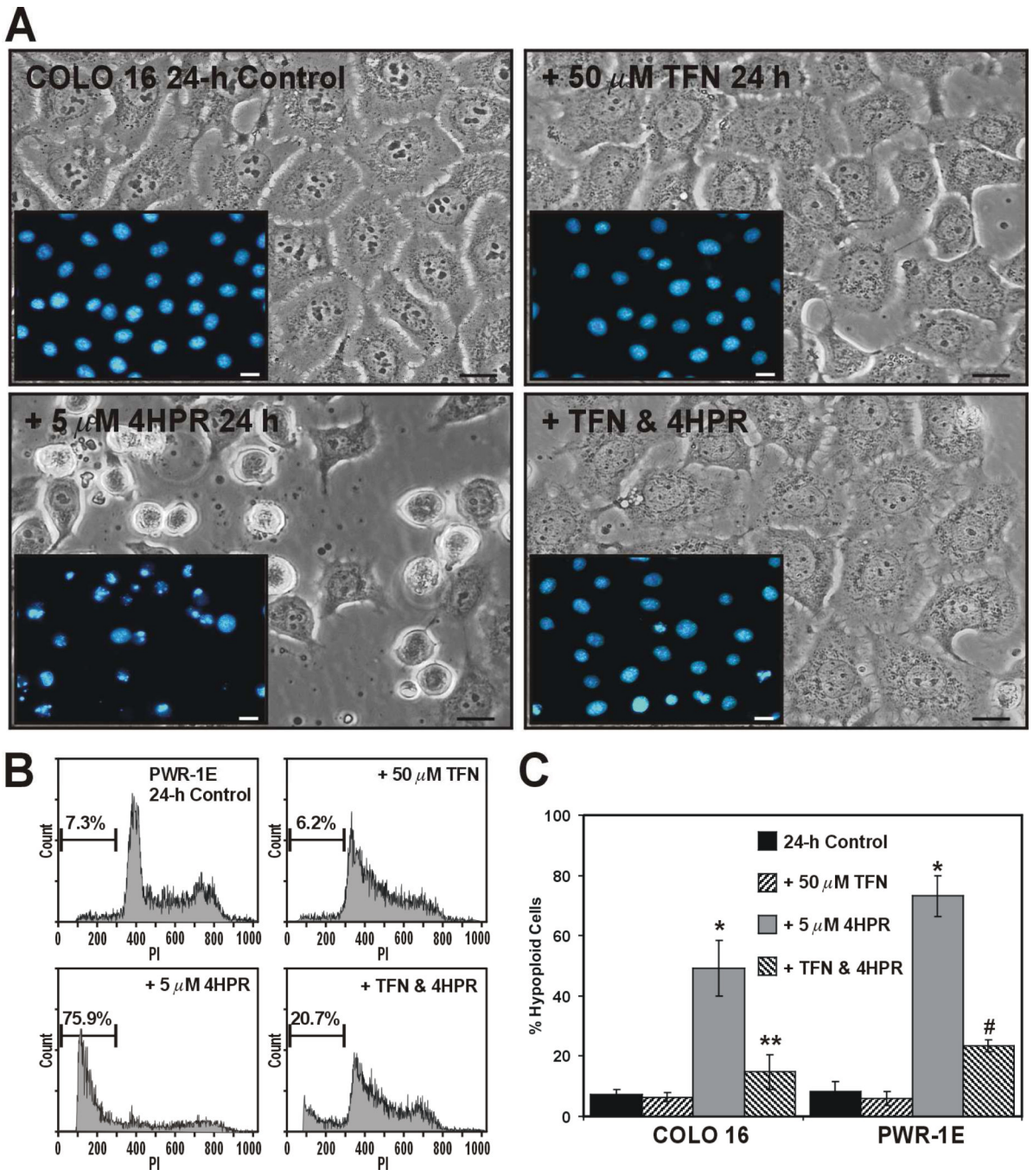

Figure 4.

TFN inhibits 4HPR-induced apoptosis in COLO 16 and PWR-1E cells. (A) Micrographs showing COLO 16 cells exposed to Me_2SO (control), 50 μM TFN, 5 μM 4HPR, or 50 μM TFN and 5 μM 4HPR for 24 h. The insets images illustrate the nuclear morphology of the COLO 16 cells as determined by Hoechst 33342 staining and epifluorescence microscopy. The scale bars equal 18 μm. *B*, Representative PI histograms showing the percent hypoploid cells for the PWR-1E cells treated as described above in (A). The gated cells detected below ~300 fluorescence units of PI on the linear *x*-axis of the representative histograms are designated the hypoploid apoptotic cell population. (C) A summary of the hypoploid cells in the treatment populations described in (A) and (B). **P*<0.001 compared to the respective controls,

**$P<0.001$ compared to the COLO 16 4HPR treatment, and #$P<0.01$ compared to the PWR-1E 4HPR treatment.

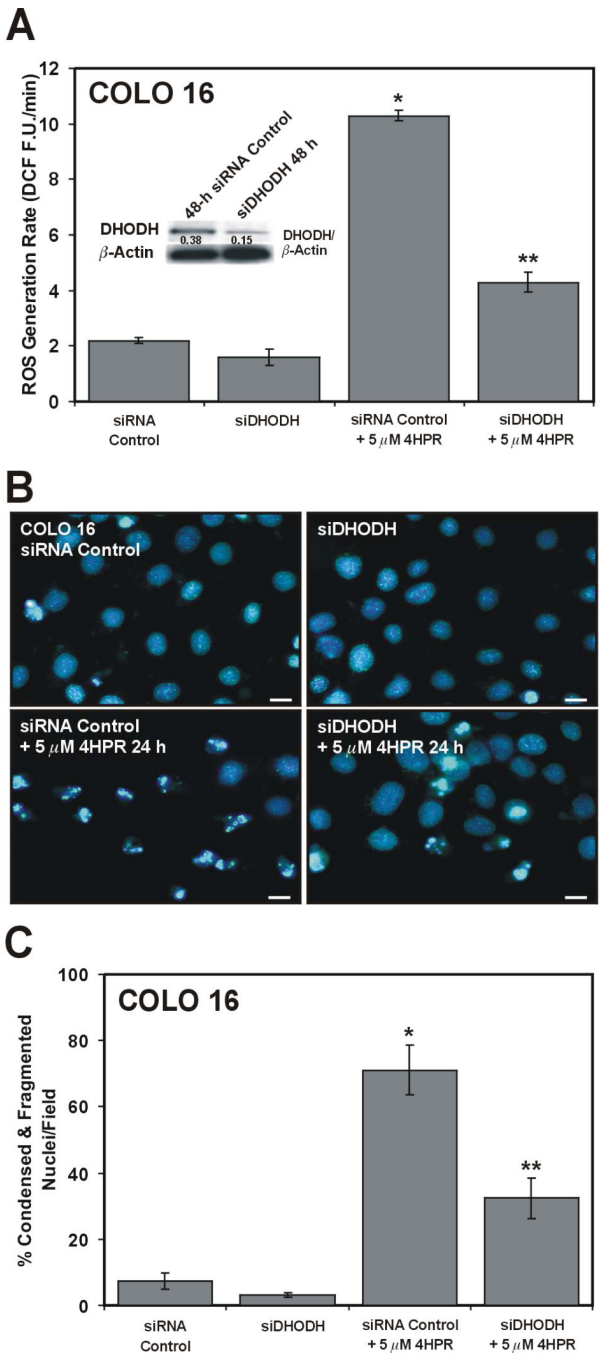

Figure 5.

DHODH RNA interference diminishes DHODH protein expression, and suppresses 4HPR-induced ROS and apoptosis in COLO 16 cells. (A) An assessment of 4HPR-induced ROS production as described in Fig. 3C following a 48-h treatments with the siRNA control or the siDHODH. **P*<0.001 compared to the siRNA control and ***P*<0.001 compared to the siRNA control with 5 μM 4HPR. The inset figure is an immunoblot analysis of DHODH expression in the COLO 16 cells following the indicated 48-h treatments. (B) Representative epifluorescence images illustrate the nuclear morphology of the COLO 16 cells treated as described in (A) for 24 h without or with 5 μM 4HPR included. The scale bars equal 18 μm. (C) A summary of the condensed/fragmented nuclei for the COLO 16 cells in the treatment

populations described in (B). *P<0.001 compared to the siRNA control and **P<0.01 compared to the siRNA control with 5 μM 4HPR.

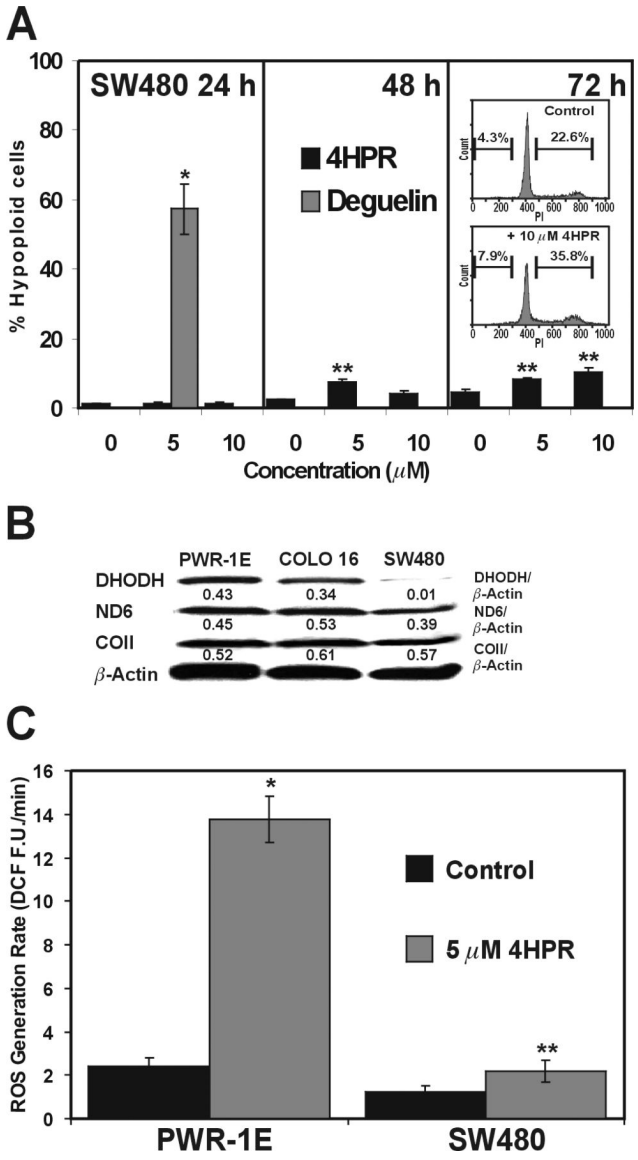

Figure 6.

Resistance to 4HPR-induced apoptosis in SW480 colon cancer cells is associated with negligible DHODH expression and 4HPR-induced ROS generation. (A) The hypoploid cells in the indicated treatments were determined by flow cytometry. **P*<0.001 compared to the 24-h control and ***P*<0.01 compared to the respective 48- and 72-h controls. (B) An immunoblot analysis of DHODH, ND6, and COII expression for the PWR-1E, COLO 16, and SW480 cells. (C) The rates of 4HPR-induced ROS generation were assessed in the PWR-1E and SW480 cells as described in Fig. 3C. **P*<0.001 compared to the PWR-1E control and ***P*<0.05 compared to the SW480 control.